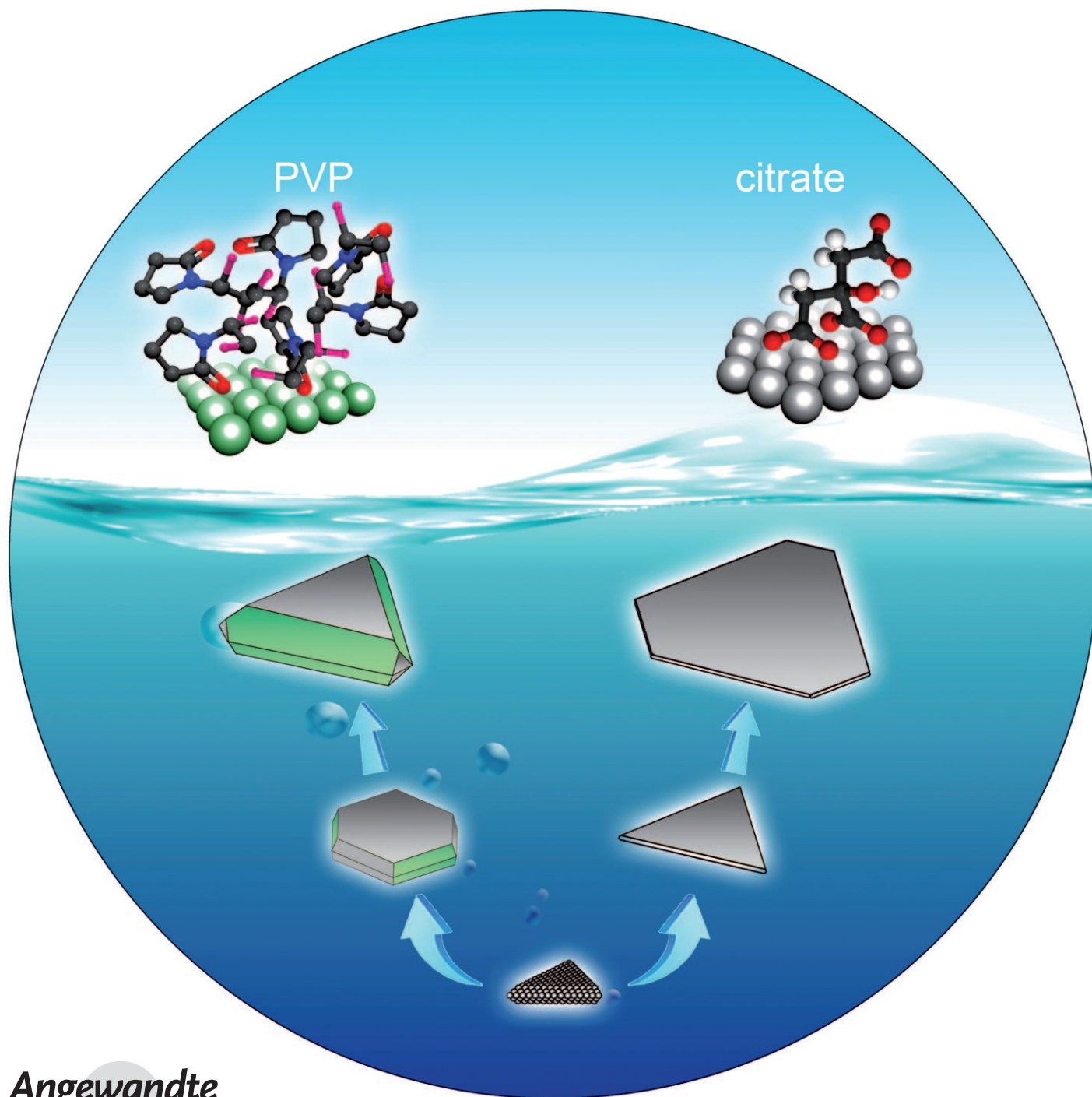


# Successive Deposition of Silver on Silver Nanoplates: Lateral versus Vertical Growth\*\*

Jie Zeng, Xiaohu Xia, Matthew Rycenga, Patrick Henneghan, Qingge Li, and Younan Xia\*



Seed-mediated growth represents a simple and robust route to nanocrystals with well-defined and controllable shapes or morphologies, and thus desired properties.<sup>[1]</sup> As a major advantage over conventional methods, introduction of pre-formed seeds into a synthesis allows growth to be disentangled from nucleation, thus making it easier to obtain a specific shape by only focusing on parameters that influence the growth. In general, the outcome of a seed-mediated synthesis is determined by the following factors:<sup>[2]</sup> 1) the difference in lattice constant between the seed and the deposited metal; 2) the internal structure of the seed, including twin defects, stacking faults, and grain boundaries; 3) the facets expressed on the seed and the presence of capping agents (e.g., surfactants, polymer stabilizers, ionic species, as well as unknown contaminants) that are capable of binding selectively to different types of facets; and 4) the reduction or growth kinetics. When oxidative etching is involved, seeds that contain twin defects could be selectively oxidized and dissolved, even before the growth process is started.<sup>[3]</sup> As a result, the shape or morphology of the final product could be completely different from that of the seeds, depending on the experimental conditions.

Seed-mediated growth has been successfully applied to a number of noble metals such as Ag, Au, Pd, Pt, and Rh, including both mono- and bimetallic systems.<sup>[4]</sup> However, manipulation and control of the evolution of shape or morphology during seed growth remains a great challenge. Recent studies have begun to address this issue by examining the growth mechanism, and its dependence on the aforementioned parameters. For example, it has been shown that twin defects or stacking faults are more reactive sites than other regions on a seed for heterogeneous nucleation, and thus lead to preferential growth parallel to the twin planes. To this end,

Au and Ag nanorods (and nanowires) with pentagonal cross-sections have been prepared from Au or Ag seeds in the form of decahedral nanocrystals.<sup>[4c,e,5]</sup> In all these cases, the newly formed Au or Ag atoms are preferentially deposited along the {111} twin planes on the seeds to generate fivefold twinned nanorods and then nanowires. It has also been demonstrated that single-crystal Ag seeds with a spherical or cubic shape can be directed to grow into nanocrystals enclosed by {111} or {100} facets by introducing citrate ions (CA) or poly(vinyl pyrrolidone) (PVP) as the capping agent.<sup>[6]</sup> In these situations, the citrate ions and PVP can bind selectively to {111} and {100} facets of Ag, respectively, to result in dominance of each type of facet in the final product. Furthermore, it has been demonstrated that the reduction kinetics can play a vital role in determining the morphology of the product of a seed-mediated growth. When single-crystal Pd nanocrystals were used as seeds, one could obtain Pd–Pt core–shell nanocrystals with a morphology similar to that of the seeds or Pd–Pt nanocrystals with dendritic arms anchored on the seeds by employing a relatively weak (e.g., citric acid) or strong (e.g., ascorbic acid) reductant for the Pt precursor.<sup>[7]</sup> Most of these studies, however, only deal with one of the four aforementioned factors. It is not clear which factor will play the most important role when more than two factors are present simultaneously. For instance, when defects and different capping agents are both involved, which of them will control the growth habit of a nanocrystal seed?

Silver (and gold) nanoplates provide an interesting model system for investigating the roles of defects and capping agents in controlling the evolution of shape or morphology. It is well known that Ag nanoplates are covered by {111} facets at both top and bottom surfaces, and contain twin planes and stacking faults on the side faces along the vertical direction.<sup>[8]</sup> Previous studies all indicate that the Ag (and Au) nanoplates would undergo lateral growth along the twin defects and stacking faults to produce larger thin plates.<sup>[8a,9]</sup> Vertical growth that can significantly increase the thickness of Ag nanoplates has not been reported to date. Even for lateral growth, this process tended to cease at a certain point, so only thin Ag plates with edge lengths below 1  $\mu\text{m}$  can be generated. Herein we demonstrate that triangular Ag nanoplates can serve as seeds for successive growth of Ag to produce plates with edge lengths (defined as the longest distance across a plate, see Figure S1 in the Supporting Information) and thicknesses that are continuously tuned from 45 nm to 5  $\mu\text{m}$  and from 5 nm to 200 nm, respectively, by confining the growth to a lateral or vertical mode. When single Ag nanospheres were deposited on the Ag plates of various thicknesses, the nanospheres showed increasingly enhanced Raman signals as the plate became thicker.

The Ag nanoplates used as seeds were prepared using a previously reported, seed-mediated protocol and their structures have been characterized in detail<sup>[10]</sup> (TEM images of a typical sample are shown in Figure S2 in the Supporting Information). It is clear that the nanoplate had a triangular cross-section along the direction perpendicular to the large, flat faces, with some slight truncation at the corners. The nanoplate is enclosed by two {111} planes as the top and bottom faces, and by round planes as the side faces. The mean

[\*] Dr. J. Zeng,<sup>[‡]</sup> X. Xia,<sup>[‡]</sup> M. Rycenga, Prof. Y. Xia


Department of Biomedical Engineering  
Washington University  
St. Louis, Missouri 63130 (USA)  
E-mail: xia@biomed.wustl.edu

X. Xia,<sup>[‡]</sup> Dr. Q. Li  
Xiamen University  
Xiamen, Fujian 361005 (People's Republic of China)

P. Henneghan  
Department of Chemistry, St. Olaf College  
Northfield, Minnesota 55057 (USA)

[†] These authors contributed equally to this work.

[\*\*] This work was supported in part by a research grant from the NSF (DMR-0804088) and startup funds from Washington University in St. Louis. Y.X. was also partially supported by the World Class University (WCU) program through the National Research Foundation of Korea funded by the Ministry of Education, Science and Technology (R32-20031). Part of the research was performed at the Nano Research Facility (NRF), a member of the National Nanotechnology Infrastructure Network (NNIN), which is funded by the NSF under award no. ECS-0335765. As a jointly supervised student, X.X. was also partially supported by a Fellowship from the China Scholarship Council. P.H. was supported by the NSF Summer Research Program in Solid-State Chemistry and Materials.

 Supporting information (detailed experimental protocols and characterization) for this article is available on the WWW under <http://dx.doi.org/10.1002/anie.201005549>.

thickness and edge length were measured to be  $(5.0 \pm 0.5)$  nm and  $(45 \pm 15)$  nm, respectively.<sup>[10b]</sup> The procedure for the epitaxial growth of Ag on the Ag nanoplates can also be repeated many times if desired (Figure S3 in the Supporting Information).

Figure 1a–e shows typical TEM and scanning electron microscopy (SEM) images of the products obtained after 1, 2, 4, 6, and 8 rounds of Ag deposition, in the presence of  $\text{Na}_3\text{CA}$  as a capping agent. In all cases, epitaxial overgrowth of Ag on the triangular Ag nanoplates generated thin plates with similar morphologies but continuously increasing edge lengths. Although each sample might contain plates with different degrees of corner truncation, we could still observe a trend of greater corner truncation with successive rounds of deposition. Although some irregular particles were observed after six rounds of deposition because of homogeneous nucleation of Ag, the yields of the nanoplates were still higher than 80%. AFM was used to determine the thickness of the nanoplates (see Figure S4 in the Supporting Information for three typical samples). As shown in Figure 1f, after nine rounds of growth, the thickness of the nanoplates increased only from  $(5.0 \pm 0.5)$  nm to  $(25 \pm 4)$  nm while the edge length increased by more than 100 times from  $(45 \pm 15)$  nm to  $(5.0 \pm 0.5)$   $\mu\text{m}$ . This result indicates that, in the presence of citrate ions, the newly formed Ag atoms were preferentially deposited on the side faces of an Ag nanoplate

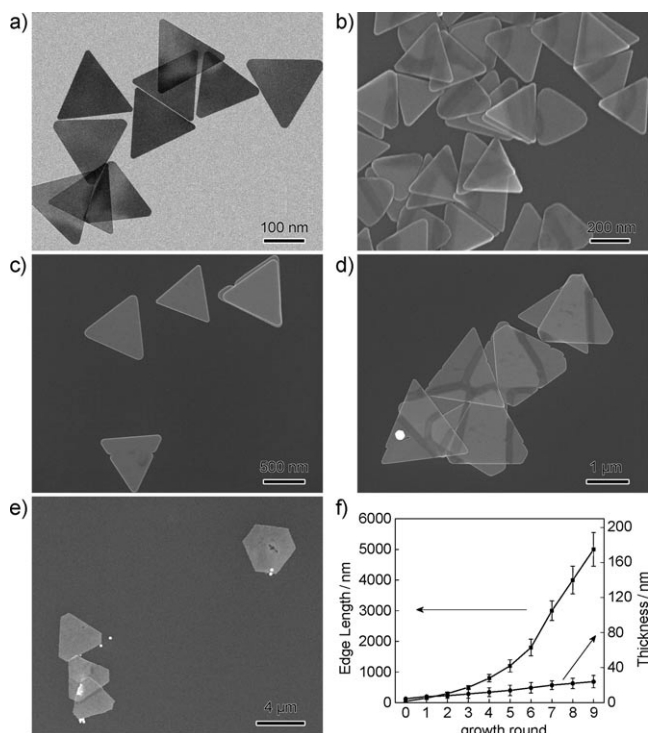


**Figure 1.** Seed-mediated growth of Ag nanoplates in the presence of  $\text{Na}_3\text{CA}$  as a capping agent. a) TEM and b–e) SEM images of Ag thin plates obtained by repeating the seeded growth 1, 2, 4, 6, and 8 times. f) Plots of edge length and thickness of the Ag nanoplates as a function of the number of growth rounds. The edge length of each sample was defined as the longest distance on a plate. Note that the length scale is considerably increased from (a) to (e).

instead of the top and bottom faces covered by  $\{111\}$  facets, thus demonstrating the feasibility of this approach for confining the growth of a nanoplate seed to the lateral directions. This argument is consistent with our previous report on the growth of Ag cubooctahedra into Ag octahedra.<sup>[6]</sup> In both cases, the  $\{111\}$  facets are expected to grow more slowly than other facets such as  $\{100\}$  during a seed-mediated growth process when  $\text{Na}_3\text{CA}$  is present. In contrast to the single-crystal cubooctahedral seeds used in our previous work,<sup>[6]</sup> the nanoplate seeds are composed of stacking faults and twin defects on the side faces, thus making them very reactive in catalyzing the reduction of Ag ions. Consequently, although  $\{111\}$  planes also exist on the side faces of a nanoplate, Ag deposition could still occur at these sites to facilitate lateral growth.

Figure 2a–e shows TEM and SEM images of the products obtained in the presence of PVP as a capping agent. In this case, the thickness of the nanoplates increased drastically from 5 nm to nearly 200 nm as the number of deposition rounds increased to nine (Figure 2f). This result suggests that the presence of PVP strongly promoted vertical growth relative to lateral growth for the deposition of Ag on the nanoplate seeds. To the best of our knowledge, all the

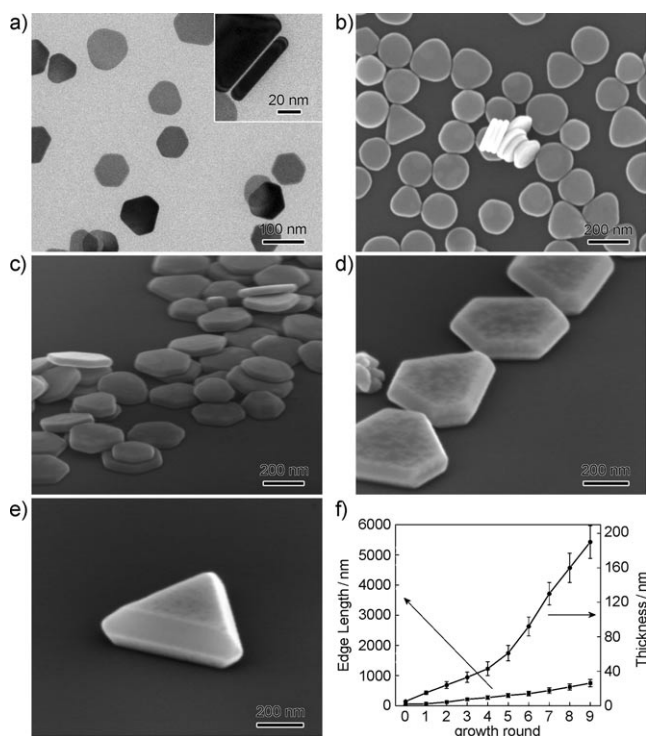


**Figure 2.** Seed-mediated growth of Ag nanoplates in the presence of PVP as a capping agent. a) TEM and b–e) SEM images of Ag nanoplates obtained by repeating the seeded growth 1, 2, 4, 6, and 8 times. The inset in (a) shows TEM image of a nanoplate standing vertically on the copper grid against one of its edges. f) Plots of edge length and thickness of Ag nanoplates as a function of the number of growth rounds. The edge length of each sample was defined as the longest distance on a plate. Note that the images in (b–e) are on the same scale and the side surface has evolved into specific facets during the vertical growth process.



previously reported methods only allowed for the syntheses of Ag nanoplates less than around 50 nm thick.<sup>[11]</sup> This work is the first demonstration of how the vertical growth of Ag nanoplates can be promoted and controlled on a scale up to 200 nm.

Our previous studies indicate that PVP binds more strongly to {100} than {111} facets of Ag and can thereby reduce the growth rate along the [100] direction, thus making the {111} facets disappear more quickly than the {100} facets.<sup>[12]</sup> Based on this argument, it is not difficult to understand why the Ag nanoplates prefer to grow vertically in the presence of PVP as a capping agent, because both the top and bottom faces of a nanoplate are terminated by {111} planes. In addition to the increase in thickness, the edge length of the products also increased to approximately 600 nm after nine rounds of repeated Ag deposition in the presence of PVP. This result indicates that there was also lateral growth arising from the presence of twin defects and stacking faults on the side faces. However, the lateral growth rate was greatly reduced to a level more or less equivalent to the rate of vertical growth because of the selectively binding of PVP to the {100} facets. During the first three rounds of deposition, the Ag nanoplates went through a truncation process, in which the shape of the nanoplate cross-section morphed from triangular for the initial seed to a hexagonal or nearly circular shape. This transition can be attributed to a thermodynamically favored growth. Such a truncation process could reduce the overall surface energy. However, as the deposition continued, the nanoplate regressed to a sharp morphology where the area ratio of the {100} to the {111} facets was gradually increased. This switch into a kinetically controlled mode is favored in the later stage of growth as it can generate a sharp morphology that has uniform facets and can be stabilized by PVP. Finally, the nanoplate grew into a thick crystal (still like a plate) similar to a truncated right bipyramid that only has a single twin plane in the middle. Considering the well-defined side facets of the thick plates, we believe that the newly deposited Ag should have crystallized in the single-crystal form without introducing additional twin defects other than the existing one in the middle of the plate along the vertical direction. It was extremely difficult (if not impossible) to obtain high-resolution TEM images from the cross-sections of these plates because the plates were too thick to be penetrated by an electron beam.

Since the experiments for both lateral and vertical growth of Ag nanoplates were performed under the same conditions, except for the use of a different capping agent, we should be able to calculate and compare the growth kinetics by calculating the deposition rate of Ag based on the volume change between two successive rounds of deposition. We found that the rate of vertical deposition for all the case of citrate was approximately one eighth of that for the case of PVP, but the rate of lateral deposition for the case of PVP was about one seventieth of that for the case of citrate. Thus, the overall growth rate for the case of PVP was much lower than that for the case of citrate. This difference can be understood by considering the self-catalytic effect of Ag seeds.<sup>[13]</sup> Specifically, Ag deposition could be catalyzed by the pre-existing Ag atoms on the faces. The catalytic activity of the

atoms at the side faces should be higher than those located on both the top and the bottom surface that were flat surfaces.

The two distinct modes of epitaxial deposition of Ag on Ag nanoplate seeds when Na<sub>3</sub>CA and PVP are used as the capping agents are summarized in Figure S5 in the Supporting Information. The facets are also indexed according to the SEM images shown in Figures 1 and 2. It is clear that during the successive deposition of Ag, the area ratio of {111} to {100} facets for the products increased in the case of Na<sub>3</sub>CA, while it decreased in the case of PVP, thus indicating orthogonal impacts for these two types of capping agents. This result is also consistent with our previous observation based on single-crystal cubooctahedral seeds.<sup>[6]</sup>

Recent studies suggest that the surface-enhanced Raman scattering (SERS) signals from Ag or Au nanoparticles could be further augmented when they were deposited on metal substrates such as evaporated thin films.<sup>[14]</sup> However, it has been difficult to experimentally determine if such an additional enhancement is dependent on the area and thickness of the metal film or not. In this regard, the as-prepared Ag plates with controllable lateral dimensions and thicknesses are attractive for this kind of study. Our experiments began with the use of Ag nanoplates having a thickness of approximately 20 nm and different edge lengths (0.5, 1, and 2  $\mu$ m). The nanoplates were placed on Si substrates, followed by the deposition of single 55 nm Ag nanospheres (Figure S6 in the Supporting Information), the surface of which had been functionalized with 1,4-benzenedithiol (1,4-BDT). The SERS spectra recorded with 514 nm laser excitation are shown in Figure 3a. All of these spectra show the characteristic SERS peaks for 1,4-BDT at 1078 cm<sup>-1</sup> and 1564 cm<sup>-1</sup>.<sup>[15]</sup> The peak at 1564 cm<sup>-1</sup> for a Ag nanosphere deposited on a Ag nanoplate with an edge length 0.5  $\mu$ m (Figure 3, curve 2) was about five times stronger than that on a Si wafer (curve 1), while the peak was two times weaker than that on Ag nanoplates with an edge length of 1 or 2  $\mu$ m (curves 3 and 4). We found that there was no obvious difference in SERS spectra for Ag nanospheres located at different regions on Ag nanoplates with an edge length of 1  $\mu$ m (Figure S7 in the Supporting Information). In addition, Ag nanoplates themselves showed very low or no SERS activities under the same measurement conditions (Figure S8 in the Supporting Information). Based on our previously reported method,<sup>[16]</sup> the SERS enhancement factors (EFs) for the 1,4-BDT coated the Ag nanospheres were calculated to be  $2.8 \times 10^5$ ,  $1.5 \times 10^6$ ,  $2.8 \times 10^6$ , and  $3.2 \times 10^6$  when deposited on Si, and on Ag plates with edge lengths of 0.5, 1, and 2  $\mu$ m, respectively.

Similarly, Ag nanoplates with an edge length of approximately 0.4  $\mu$ m and thicknesses of 18, 55, and 100 nm were also used as the underlying substrate for measuring the SERS EFs for single 55 nm Ag nanospheres. Figure 3b shows SERS spectra taken from the 1,4-BDT-coated Ag nanospheres deposited on such Ag nanoplates. In these cases, the peak at 1564 cm<sup>-1</sup> for a Ag nanosphere deposited on a 55 nm thick Ag nanoplate (Figure 3b, curve 6) was about six times stronger than that on a 18 nm thick Ag nanoplate, and almost the same as that on a 100 nm thick Ag nanoplate. The SERS EFs for the 1,4-BDT-coated Ag nanospheres were calculated to be  $1.5 \times 10^6$ ,  $9.4 \times 10^6$ , and  $1.1 \times 10^7$  when they

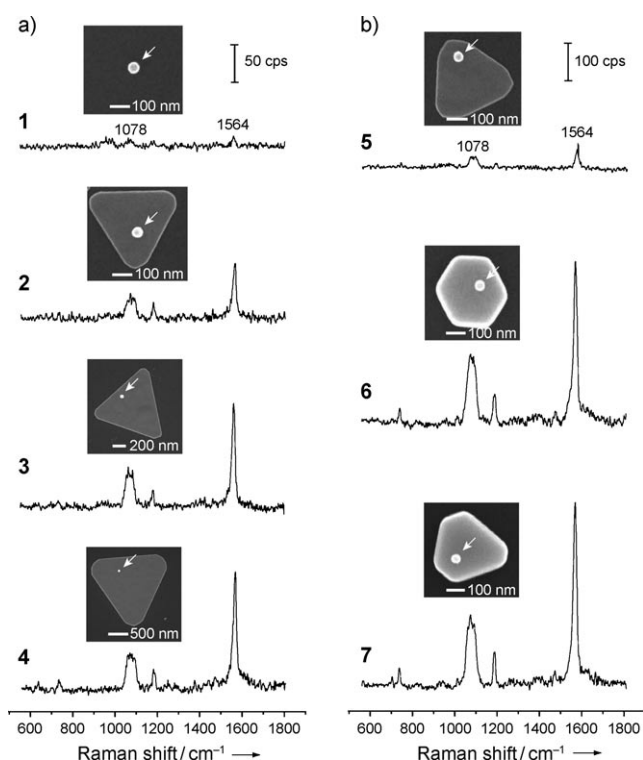


**Figure 3.** Comparison of SERS spectra taken from single 1,4-BDT-coated Ag nanospheres (55 nm in diameter) deposited on Ag nanoplates with different edge lengths (a) and thicknesses (b) respectively. a) The Ag nanospheres were deposited on 1) Si wafer, and on Ag nanoplates with edge lengths of 2) 0.5, 3) 1, and 4) 2  $\mu\text{m}$ . b) The Ag nanospheres were deposited on Ag nanoplates with thicknesses of 5) 18, 6) 50, and 7) 100 nm. The SEM image above each spectrum denotes the corresponding structure. Note that the SERS signals in (a) and (b) are on different scales, and length scales in (2–4) are different. The peak at  $1078\text{ cm}^{-1}$  arises from a combination of the phenyl ring breathing mode, C–H in-plane bending, and C–S stretching, and the peak at  $1564\text{ cm}^{-1}$  can be assigned to phenyl ring stretching motion (8a vibrational mode).<sup>[15]</sup> The weak broad band in the range of  $900\text{--}1000\text{ cm}^{-1}$  arises from the Si substrate. cps = counts per second.

were deposited on 18, 55, and 100 nm thick Ag nanoplates, respectively. These experimental data clearly show that the SERS EFs for Ag nanospheres indeed have a strong dependence on the thickness of the underlying metal substrate, as is consistent with theoretical calculations.<sup>[17]</sup> Interestingly, once the thickness of the Ag nanoplate had increased to a value that was larger than the diameter of the Ag nanosphere, the EF would reach a saturated value. The SERS EFs had no strong dependence on the area or edge length of the Ag nanoplates, at least in the range of  $0.5\text{--}2\text{ }\mu\text{m}$ .

In summary, we have demonstrated that Ag nanoplates could grow in a lateral or vertical mode depending on the capping agent present in the solution. When  $\text{Na}_3\text{CA}$  was added, lateral growth was more favorable and thus the formation of Ag thin plates with large lateral dimensions. In contrast, thicker Ag plates were obtained because of vertical growth when  $\text{Na}_3\text{CA}$  was substituted with PVP. This sharp difference observed in the course of Ag deposition can be attributed to the different affinities of  $\text{Na}_3\text{CA}$  and PVP

towards  $\{111\}$  and  $\{100\}$  facets of Ag. These results not only provide new insights into the mechanistic understanding of seed-mediated growth, but also offer a versatile route to Ag nanocrystals with well-defined and controllable dimensions and shapes (or facets) for various applications.

Received: September 4, 2010

Published online: October 29, 2010

**Keywords:** nanostructures · seeded growth · silver · surface capping · surface-enhanced Raman spectroscopy

- [1] a) R. Jin, Y. C. Cao, E. Hao, G. S. Metraux, G. C. Schatz, C. A. Mirkin, *Nature* **2003**, 425, 487; b) B. Nikoobakht, M. A. El-Sayed, *Chem. Mater.* **2003**, 15, 1957; c) Y. Xia, Y. Xiong, B. Lim, S. E. Skrabalak, *Angew. Chem.* **2009**, 121, 62; *Angew. Chem. Int. Ed.* **2009**, 48, 60.
- [2] a) X. Liu, Y. Zhang, D. K. Goswami, J. S. Okasinski, K. Salaita, M. J. Bedzyk, C. A. Mirkin, *Science* **2005**, 307, 1763; b) N. R. Jana, L. Gearheart, C. J. Murphy, *Adv. Mater.* **2001**, 13, 1389; c) J. M. Petroski, Z. L. Wang, T. C. Green, M. A. El-Sayed, *J. Phys. Chem. B* **1998**, 102, 3316; d) T. S. Ahmadi, Z. L. Wang, T. C. Green, A. Henglein, M. A. El-Sayed, *Science* **1996**, 272, 1924.
- [3] a) B. Wiley, T. Herricks, Y. Sun, Y. Xia, *Nano Lett.* **2004**, 4, 1733; b) Y. Xiong, J. Chen, B. Wiley, Y. Xia, S. Aloni, Y. Yin, *J. Am. Chem. Soc.* **2005**, 127, 7332; c) B. J. Wiley, Y. Chen, J. M. McLellan, Y. Xiong, Z. Y. Li, D. Ginger, Y. Xia, *Nano Lett.* **2007**, 7, 1032.
- [4] a) S. E. Habas, H. Lee, V. Radmilovic, G. A. Somorjai, P. Yang, *Nat. Mater.* **2007**, 6, 692; b) F. R. Fan, D. Y. Liu, Y. F. Wu, S. Duan, Z. X. Xie, Z. Y. Jiang, Z. Q. Tian, *J. Am. Chem. Soc.* **2008**, 130, 6949; c) D. Seo, C. I. Yoo, J. Jung, H. Song, *J. Am. Chem. Soc.* **2008**, 130, 2940; d) A. Tao, P. Sinsermsuksakul, P. Yang, *Angew. Chem.* **2006**, 118, 4713; *Angew. Chem. Int. Ed.* **2006**, 45, 4597; e) N. R. Jana, L. Gearheart, C. J. Murphy, *J. Phys. Chem. B* **2001**, 105, 4065; f) H. Yu, P. C. Gibbons, K. F. Kelton, W. E. Buhro, *J. Am. Chem. Soc.* **2001**, 123, 9198.
- [5] a) N. R. Jana, L. Gearheart, C. J. Murphy, *Chem. Commun.* **2001**, 617; b) B. Pietrobon, M. McEachran, V. Kitaev, *ACS Nano* **2009**, 3, 21.
- [6] J. Zeng, Y. Zheng, M. Rycenga, J. Tao, Z. Y. Li, Q. Zhang, Y. Zhu, Y. Xia, *J. Am. Chem. Soc.* **2010**, 132, 8552.
- [7] a) B. Lim, J. Wang, P. H. Camargo, M. Jiang, M. J. Kim, Y. Xia, *Nano Lett.* **2008**, 8, 2535; b) B. Lim, M. Jiang, P. H. Camargo, E. C. Cho, J. Tao, X. Lu, Y. Zhu, Y. Xia, *Science* **2009**, 324, 1302.
- [8] a) R. Jin, Y. Cao, C. A. Mirkin, K. L. Kelly, G. C. Schatz, J. G. Zheng, *Science* **2001**, 294, 1901; b) S. Chen, D. L. Carroll, *Nano Lett.* **2002**, 2, 1003.
- [9] a) K. L. Shuford, M. A. Ratner, G. C. Schatz, *J. Chem. Phys.* **2005**, 123, 114713; b) J. E. Millstone, G. S. Métraux, C. A. Mirkin, *Adv. Funct. Mater.* **2006**, 16, 1209.
- [10] a) V. Shrotriya, G. Li, Y. Yao, T. Moriarty, K. Emery, Y. Yang, *Adv. Funct. Mater.* **2006**, 16, 2016; b) J. Zeng, S. Roberts, Y. Xia, *Chem. Eur. J.* **2010**, DOI: 10.1002/chem.201002665.
- [11] a) J. E. Millstone, S. J. Hurst, G. S. Métraux, J. I. Cutler, C. A. Mirkin, *Small* **2009**, 5, 646; b) S. H. Chen, D. L. Carroll, *J. Phys. Chem. B* **2004**, 108, 5500; c) A. Callegari, D. Tonti, M. Chergui, *Nano Lett.* **2003**, 3, 1565; d) I. Pastoriza-Santos, L. M. Liz-Marzán, *Nano Lett.* **2002**, 2, 903.
- [12] a) D. S. Kilin, O. V. Prezhdo, Y. Xia, *Chem. Phys. Lett.* **2008**, 458, 113; b) Y. Sun, B. Mayers, Y. Xia, *Nano Lett.* **2003**, 3, 675.
- [13] a) J. Zeng, J. Huang, C. Liu, C. Wu, Y. Lin, X. Wang, S. Zhang, J. G. Hou, Y. Xia, *Adv. Mater.* **2010**, 22, 1936; b) A. Gole, C. J. Murphy, *Chem. Mater.* **2004**, 16, 3633.

- [14] a) D. J. Anderson, M. Moskovits, *J. Phys. Chem. B* **2006**, *110*, 13722; b) K. Kim, J. K. Yoon, *J. Phys. Chem. B* **2005**, *109*, 20731; c) J. K. Daniels, G. Chumanov, *J. Phys. Chem. B* **2005**, *109*, 17936; d) M. K. Kinnan, G. Chumanov, *J. Phys. Chem. C* **2007**, *111*, 18010.
- [15] a) M. A. Khan, T. P. Hogan, S. Shanker, *J. Raman Spectrosc.* **2008**, *39*, 893; b) G. Sauer, G. Brehm, S. Schneider, *J. Raman Spectrosc.* **2004**, *35*, 568.
- [16] a) P. H. C. Camargo, M. Rycenga, L. Au, Y. Xia, *Angew. Chem.* **2009**, *121*, 2214; *Angew. Chem. Int. Ed.* **2009**, *48*, 2180; b) J. M. McLellan, Z. Y. Li, A. R. Siekkinen, Y. Xia, *Nano Lett.* **2007**, *7*, 1013.
- [17] F. Le, N. Z. Lwin, J. M. Steele, M. Käll, N. J. Halas, P. Nordlander, *Nano Lett.* **2005**, *5*, 2009.
-